

Modeling liquid thermal explosion reactor containing *tert*-butyl peroxybenzoate

Chun-Ping Lin · Jo-Ming Tseng · Yi-Ming Chang ·
Shang-Hao Liu · Yen-Chun Cheng ·
Chi-Min Shu

NATAS2009 Special Issue
© Akadémiai Kiadó, Budapest, Hungary 2010

Abstract This study investigated the role played by green thermal analysis technology in promoting the use of resources, preventing pollution, reducing energy consumption and protecting the environment. The chemical *tert*-butyl peroxybenzoate (TBPB) has been widely employed in the petrifaction industries as an initiator of polymerization formation agent. This study established the thermokinetic parameters and thermal explosion hazard for a reactor containing TBPB via differential scanning calorimetry (DSC). To simulate thermokinetic parameters, a 5-ton barrel reactor of liquid thermal explosion model was created in this study. The approach was to develop a precise and effective procedure on thermal decomposition, runaway, and thermal hazard properties, such as activation energy (E_a), control temperature (CT), critical temperature (TCR), emergency temperature (ET), heat of decomposition (ΔH_d), self-accelerating decomposition temperature ($SADT$), time to conversion limit (TCL), total energy release (TER), time to maximum rate under isothermal

condition (TMR_{iso}), etc. for a reactor containing TBPB. Experimental results established the features of thermal decomposition and huge size explosion hazard of TBPB that could be executed as a reduction of energy potential and storage conditions in view of loss prevention.

Keywords Differential scanning calorimetry (DSC) · Green thermal analysis technology · Liquid thermal explosion · *Tert*-butyl peroxybenzoate · Thermal explosion hazard

List of symbols

A	Pre-exponential factor (s^{-1})
C_p	Specific heat capacity ($J\ kg^{-1}\ m^{-3}$)
CT	Control temperature ($^{\circ}C$)
E_a	Activation energy ($kJ\ mol^{-1}$)
E_1	Activation energy of the 1st stage ($kJ\ mol^{-1}$)
E_2	Activation energy of the 2nd stage ($kJ\ mol^{-1}$)
ET	Emergency temperature ($^{\circ}C$)
E_{xi}	Activation energy at isoconversional degree xi ($kJ\ mol^{-1}$); $i = 1, 2, 3, 4$
f_i	Kinetic functions of the i th stage ($i = 1, 2, 3$)
$f(\alpha)$	Kinetic functions
k_0	Pre-exponential factor ($m^3\ mol^{-1}\ s^{-1}$)
k_i	Reaction rate constant ($mol\ L^{-1}\ s^{-1}$); $i = 1, 2$
L	Characteristic dimension (m)
n	Reaction order or unit outer normal on the boundary (dimensionless)
NC	Number of components (dimensionless)
n_i	Reaction order of the i th stage (dimensionless); $i = 1, 2, 3$
Q_i	Reaction calorific effect ($J\ g^{-1}$)
Q_t	Heat production rate ($kJ\ g^{-1}\ min^{-1}$)
Q_0	Heat production ($kJ\ kg^{-1}$)

C.-P. Lin
Department of Health and Nutrition Biotechnology,
College of Health Science, Asia University, 500, Lioufeng Rd.,
Wufeng, Taichung 41354, Taiwan, ROC

J.-M. Tseng
Institute of Safety and Disaster Prevention Technology,
Central Taiwan University of Science and Technology, 666,
Buzih Rd., Beitun District, Taichung 40601, Taiwan, ROC

Y.-M. Chang · S.-H. Liu · Y.-C. Cheng · C.-M. Shu (✉)
Process Safety and Disaster Prevention Laboratory,
Department of Safety, Health, and Environmental Engineering,
National Yunlin University of Science and Technology
(NYUST), 123, University Rd., Sec. 3, Douliou 64002,
Yunlin, Taiwan, ROC
e-mail: shucm@yuntech.edu.tw

Q_i^∞	Specific heat effect of a reaction (J kg^{-1})
q	Heat flow (J g^{-1})
R	Gas constant ($8.31415 \text{ J K}^{-1} \text{ mol}^{-1}$)
r_i	Reaction rate of the i th stage (g s^{-1}); $i = 1, 2, 3, 4$
S	Heat-exchange surface (m^2)
$SADT$	Self-accelerating decomposition temperature ($^\circ\text{C}$)
T	Absolute temperature (K)
T_0	Exothermic onset temperature ($^\circ\text{C}$)
T_c	Critical temperature ($^\circ\text{C}$)
TCL	Time to conversion limit (day)
TCR	Critical temperature ($^\circ\text{C}$)
TER	Total energy release (kJ kg^{-1})
T_e	Ambient temperature ($^\circ\text{C}$)
T_f	Exothermic final temperature ($^\circ\text{C}$)
TMR_{iso}	Time to maximum rate under isothermal condition (min)
T_p	Peak temperature ($^\circ\text{C}$)
T_{p_i}	Peak temperature of different scanning rates ($^\circ\text{C}$); $i = 1, 2, 3, 4$
T_{α_i}	Different temperature in various scanning rates at isoconversional degree α_i ; $i = 1, 2, 3, 4$
T_{wall}	Temperature on the wall ($^\circ\text{C}$)
t	Time (s)
W	Heat power (W g^{-1})
z	Autocatalytic constant (dimensionless)
α	Degree of conversion (dimensionless)
α_i	Isoconversion degree in various scanning rates by Ozawa–Flynn–Wall kinetic equation (dimensionless); $i = 1, 2, 4, 10$
β	Scanning rate ($^\circ\text{C min}^{-1}$)
β_i	Scanning rate ($^\circ\text{C min}^{-1}$); $i = 1, 2, 3, 4$
γ	Degree of conversion (dimensionless)
ρ	Density (kg m^{-3})
λ	Thermal conductivity ($\text{W m}^{-1} \text{ K}^{-1}$)
δ	Shape factor (dimensionless)
χ	Heat transfer coefficient ($\text{W m}^{-2} \text{ K}^{-1}$)
ΔH_d	Heat of decomposition (kJ kg^{-1})

Introduction

Tert-butyl peroxybenzoate (TBPB) is the most widely applied chemical in the polymerization of styrene, acrylates, methacrylates, ethylene, and in cross-linking peroxides. TBPB can be used for polymerization and copolymerization for styrene in the temperature range of 100–140 $^\circ\text{C}$. In other manufacturing processes, the operating temperature is prominently higher. TBPB decomposes quickly upon heating and under influence of light, resulting in fire and explosion hazard [1, 2]. Thus, TBPB should be stored in containers that conform to the criteria of National Fire Protection Association (NFPA) [2].

Furthermore, the aim of this study was to appraise thermal experimental data of TBPB via differential scanning calorimetry (DSC) [3, 4], by applying the well-known Kissinger kinetic equation [5] and Ozawa–Flynn–Wall kinetic equation [6–10] at various scanning rates (1, 2, 4, and 10 $^\circ\text{C min}^{-1}$), and then to compare kinetics evaluation simulation [11]. This study was associated with a comparison of the mathematical and simulation approaches to build up a precise and effective procedure on thermokinetic parameters of thermal decomposition properties for TBPB, and then executed to simulate liquid thermal hazard [11].

Traditionally, the thermal hazard parameters of organic peroxides were evaluated such that the self-accelerating decomposition temperature ($SADT$) is the lowest ambient temperature at which the temperature increase of a chemical substance is at least 6 K in a specified commercial package during a period of 7 days or less by the United Nations (UN) recommendations [12–14]. The UN published recommendations concerning the safe transport of dangerous goods to avoid adverse incidents [12–14]. The $SADT$ is a very crucial parameter for assessing the safety management of reactive substances in storage and transportation. $SADT$ is generally determined by one of four testing methods recommended by the UN orange book: the United States $SADT$ test, the adiabatic storage test, the isothermal storage test, and the heat accumulation storage test [15–17]. There are significant disadvantages in these four methods for green thermal analysis technology with regard to promoting the use of resources, preventing pollution, reducing energy consumption, and protecting the environment.

The most commonly used tests by the UN and the United States are $SADT$ tests for organic peroxides, such as 0.5 L Dewar vessel, 25 kg package, and 55 gallon container, but this study simulated the method for thermal hazard evaluation. Specific testing schemes are described there, to identify and classify dangerous goods of different classes and divisions. Actually, it is impossible to truly test a 5-ton reactor or storage container, which is difficult and dangerous for $SADT$ tests, but through a simulated method on thermal hazard evaluation of organic peroxides, it can be processed.

Famous scientists, such as Fisher and Goetz [15, 16], Whitmore and Wilberforce [17, 18], Malow and Wehrstedt [19], Kotoyori [20], Sun et al. [21], Yang et al. [22], Yu and Hasegawa [23], Li and Hasegawa [24], Hordijk and Groot [25], Roduit et al. [26], etc., have already developed more convenient estimation methods, such as $SADT$ tests for the organic peroxides or energetic materials, and TBPB's $SADT$ tests were created too. In fact, the situation is very dangerous while the organic peroxides are stored in the huge containers. This will be proved again via our thermal hazard simulation.

Moreover, this study allows estimation of runaway parameters at the earliest stages of the life cycle of TBPB's

product, thus ensuring elimination or significant reduction of the necessity of thermal hazardous experiments. These approaches can be used for many important tasks, such as conceptual design and optimization of chemical processes, reactor design, assessment of reaction hazards, choice of safer conditions of storage and transportation of a commercial chemical, to name a few. The approach also was to build up a green technology on thermal decomposition and hazard properties, such as activation energy (E_a), control temperature (CT), critical temperature (TCR), emergency temperature (ET), heat of decomposition (ΔH_d), $SADT$, time to conversion limit (TCL), total energy release (TER), and time to maximum rate under isothermal condition (TMR_{iso}), etc., for a reactor containing TBPB.

Experimental and methods

Samples

Tert-butyl peroxybenzoate (TBPB) of 98 mass%, a light yellow liquid, was purchased from Akzo Nobel Ltd. [1], and then stored in a refrigerator at 4 °C.

Differential scanning calorimetry tests

Samples of TBPB were tested on a Mettler TA8000 system coupled with a DSC 821^e measuring test crucible (Mettler ME-26732), which is the essential part of the experiment. It was used for carrying out the experiments for withstanding relatively high pressure to approximately 100 bar. STAR^e software was used to obtain thermal curves [3]. Before the experiment, a blank experiment should be done; after the blank experiment, only then should the sample test be started. The scanning rates selected for the temperature-programmed ramp were 1, 2, 4, and 10 °C min⁻¹. Roughly, 4–5 mg of the sample was used for acquiring the experimental data. As far as the test cells are concerned, these gold-plated high-pressure crucibles (40 μ L), which can be pressed together, have proven to be very useful for safety investigation, but they can only be used for one measurement with a maximum pressure of 15 MPa. The lid is pressed onto the crucible with a pressure of about a ton; therefore, the seal tightens the crucible. A toggle press is applied to close the crucible. The test cell was sealed manually by a special tool equipped with Mettler's DSC. The range of temperature rise was chosen from 30 to 300 °C for TBPB 98 mass%.

Reaction kinetic model simulations

The experimental data were processed, and the kinetics evaluated by applying thermal safety software (TSS) [11].

Liquid thermal explosion simulation

The method is thoroughly described by TSS for a liquid thermal explosion model and the algorithms that are used [11, 27]. The experimental setup was based upon TBPB's storage container. The reactor is barrel shaped, the total weight is ca. 5 tons (4,500 L), the radius is 1 m, the height is 2 m, and the shell thickness is 0.1 m. The reactor had the following properties: $C_P = 2,000 \text{ J kg}^{-1} \text{ m}^{-3}$, $\lambda = 0.5 \text{ W m}^{-1} \text{ K}^{-1}$. The heat exchange on the boundary is given by the condition of the third kind (Newton's law): the ambient temperature $T_e = 20 \text{ }^\circ\text{C}$, the heat transfer coefficient $\chi = 10 \text{ W m}^{-2} \text{ K}^{-1}$. The condition bound of ambient temperature was as follows: the reactor seal is ca. 37 °C under room temperature in summer but is ca. 60 °C in outdoor exposure under sunlight, the overheating environment temperature is 120 °C, and the temperature for the scene of a fire is 250 °C.

Results and discussion

Kissinger kinetic equation

The Kissinger formal model can be expressed on the basis of scanning rate and peak temperature that may consist of several dependent equations as illustrated by Eq. 1 [5]:

$$\ln\left(\frac{\beta}{T_p^2}\right) = \ln\frac{AR}{E_a} - \frac{E_a}{RT_p} \quad (1)$$

where β is the scanning rate; T_p is the peak temperature; A is the pre-exponential factor; E_a is the activation energy; and R is the gas constant [5].

The DSC thermal analysis for TBPB's thermal decomposition at scanning rates of 1, 2, 4, and 10 °C min⁻¹ via STAR^e is listed in Table 1, and thermal analysis curves are shown in Figs. 1 and 2. The analysis graphs on E_a for TBPB with various scanning rates of 1, 2, 4, and 10 °C min⁻¹ by the Kissinger kinetic equation are illustrated in Fig. 3. The E_a , the correlation coefficient (R^2), and the standard deviation, which were computed by the kinetic equation, are 107 kJ mol⁻¹, 0.97626, and 0.15713, respectively.

Ozawa–Flynn–Wall kinetic equation

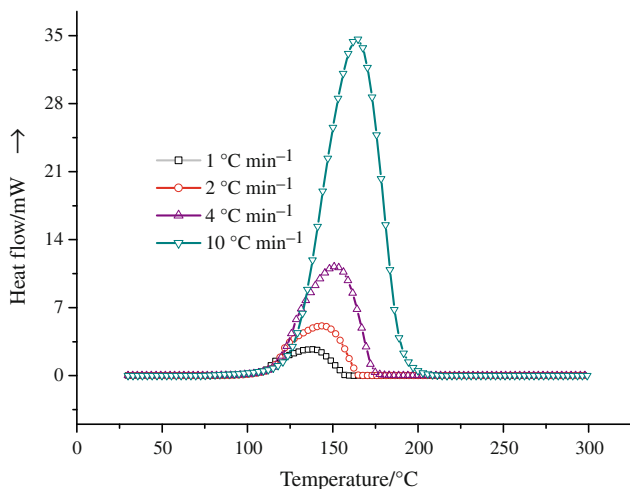
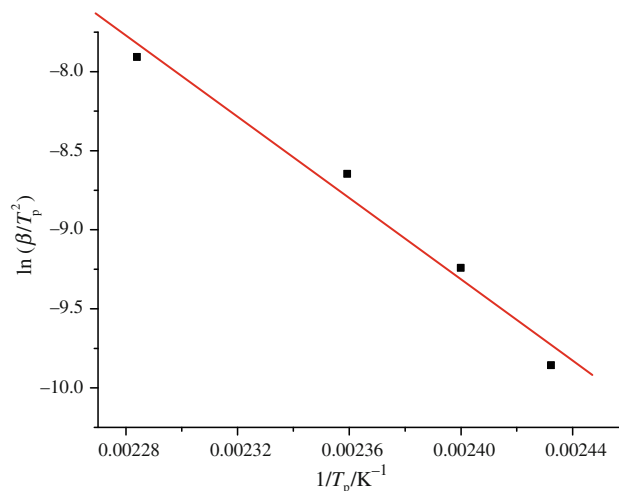
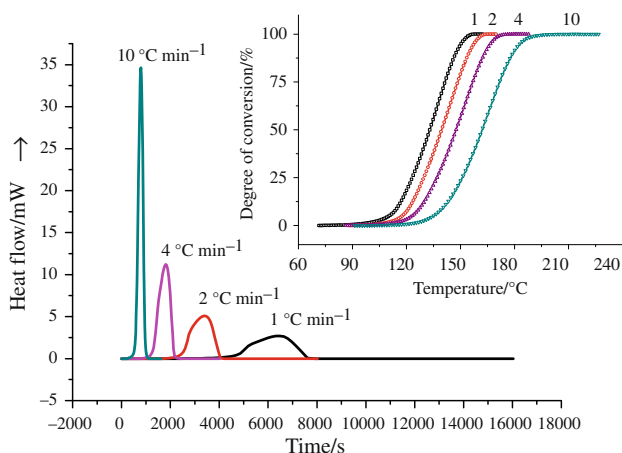
Formal models can be described based on the scanning rate that may consist of several dependent equations as illustrated by Eq. 2 [6–10].

$$\ln\beta = -1.0516\frac{E_a}{RT_{ai}} + \text{const.} \quad (2)$$

At the different scanning rates under isoconversional degree condition, a set of kinetic equations can be derived [4–8].

Table 1 Experimental data for TBPB's thermal decompositions via STAR^e software by DSC tests

$\beta/^\circ\text{C min}^{-1}$	$T_0/^\circ\text{C}$	$T_p/^\circ\text{C}$	$T_f/^\circ\text{C}$	Maximum heat flow/mW	$\ln k_0/\ln (\text{s}^{-1})$	n	$E_a/\text{kJ mol}^{-1}$	$\Delta H_d/\text{kJ kg}^{-1}$
1	65.1	138.1	165.0	2.71	12.42	0.59	66.46	1,237.49
2	87.7	143.6	173.1	5.11	11.68	0.58	63.10	1,253.33
4	79.2	150.8	191.3	11.22	16.22	0.81	77.06	1,404.66
10	66.8	164.8	219.8	34.65	19.52	0.91	87.82	1,125.99

**Fig. 1** DSC thermal curves of heat flow versus temperature for TBPB decomposition at scanning rates of 1, 2, 4, and 10 °C min⁻¹**Fig. 3** Activation energy analysis graph for TBPB with various scanning rates of 1, 2, 4, and 10 °C min⁻¹ by Kissinger kinetic equation**Fig. 2** DSC thermal curves of heat flow versus time and α versus temperature for TBPB decomposition at scanning rates of 1, 2, 4, and 10 °C min⁻¹

$$\begin{aligned}
 \ln \beta_1 + 1.0516 \frac{E_{ai}}{RT_{a1}} &= \ln \beta_2 + 1.0516 \frac{E_{ai}}{RT_{a2}} \\
 &= \ln \beta_3 + 1.0516 \frac{E_{ai}}{RT_{a3}} \\
 &= \ln \beta_4 + 1.0516 \frac{E_{ai}}{RT_{a4}} = \dots \quad (3)
 \end{aligned}$$

where β_1 , β_2 , β_3 , and β_4 are different scanning rates, E_{ai} is the activation energy at isoconversional degree α_i ; $T_{\alpha 1}$, $T_{\alpha 2}$, $T_{\alpha 3}$, and $T_{\alpha 4}$ are different temperatures in various scanning rates at isoconversional degree α_i .

TBPB's activation energy analysis graphs at scanning rates of 1, 2, 4, and 10 °C min⁻¹ under isoconversional degree at 1, 10, 20, 30, 40, and 50% (isoconversional degree under less than at T_p condition) by kinetic equation are illustrated in Fig. 4; the thermokinetic parameters of thermal decomposition are listed in Table 2.

The famous kinetic equations have one of the most critical points in thermal analysis investigation, which is the establishment of a reaction kinetic model based on the thermal decomposition, scanning rate, peak temperature, and constants of conversion such as Kissinger and Ozawa–Flynn–Wall [6–10]. As far as thermal decomposition is concerned, the corresponding E_a was calculated by DSC experimental data.

Therefore, the kinetic equations provided an easy, quick, and straightforward mathematical model for analyzing the E_a of TBPB. Particularly, TBPB's thermal decomposition belongs to either a chain reaction or n th order reaction; strictly from STAR^e, Kissinger, and Ozawa–Flynn–Wall

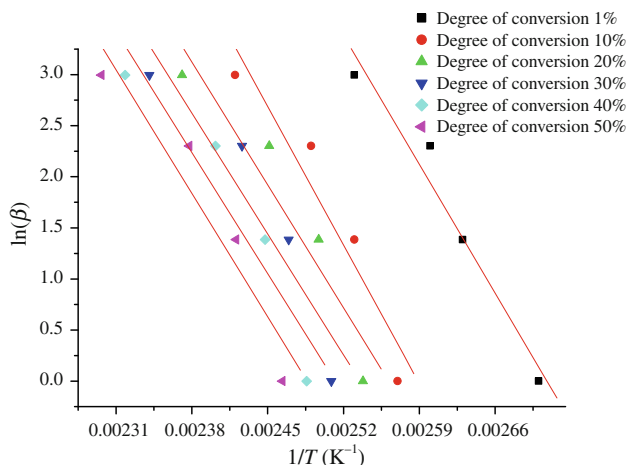


Fig. 4 Activation energy analysis graphs for TBPB at scanning rates of 1, 2, 4, and 10 °C min⁻¹ under α at 1, 10, 20, 30, 40, and 50% by Ozawa–Flynn–Wall kinetic equation

Table 2 TBPB’s thermokinetic parameters for the thermal decompositions in various degrees of conversion 1, 10, 20, 30, 40, and 50% by Ozawa–Flynn–Wall kinetic equation

Sample	TBPB		
	E_a /kJ mol ⁻¹	Correlation coefficient, R^2	Standard deviation
1	106	0.98702	0.13731
10	117	0.99481	0.08687
20	109	0.98929	0.12465
30	107	0.98381	0.15332
40	107	0.98609	0.14216
50	109	0.99032	0.11855
Average	109	N/A	N/A

kinetic equations, it remains an unknown topic [3, 5–10]. Furthermore, TBPB is required to conduct by other approaches, and then with the assessed results of thermokinetic parameters compared in the future.

Reaction kinetic model simulations

The kinetic model of simulation can represent complex multi-stage reactions that may consist of several independent, parallel, and consecutive stages, as illustrated by the following formats [11].

Simple single-stage reaction:

$$\frac{d\alpha}{dt} = k_0 e^{-\frac{E_a}{RT}} f(\alpha) \tag{4}$$

One-stage for n th order reaction:

Table 3 Thermokinetic parameters evaluated by n th order simulation

Sample	TBPB			
	1	2	4	10
$\ln k_0/\ln s^{-1}$	26.54	26.15	26.00	26.48
E_a /kJ mol ⁻¹	112.83	111.11	110.40	112.57
n	1.04	1.05	1.07	1.14
ΔH_d /kJ kg ⁻¹	1,244.16	1,271.30	1,415.20	1,132.06

$$\frac{d\alpha}{dt} = k_0 e^{-\frac{E_a}{RT}} (1 - \alpha)^n \tag{5}$$

Multistage for autocatalytic reaction:

$$f(\alpha) = (1 - \alpha)^{n_1} (\alpha^{n_2} + z) \tag{6}$$

where E_a is the activation energy; k_0 is the pre-exponential factor; z is the autocatalytic constant; and n_1 and n_2 are reaction orders of a specific stage [11]. Reaction which includes two consecutive stages:

$$\frac{d\alpha}{dt} = k_1 e^{-\frac{E_1}{RT}} (1 - \alpha)^{n_1}; \quad \frac{d\gamma}{dt} = k_2 e^{-\frac{E_2}{RT}} (\alpha - \gamma)^{n_2} \tag{7}$$

where α and γ are conversions of the reactant A and product C, respectively; and E_1 and E_2 are activation energies of stages one and two. Two parallel reactions are full autocatalysis:

$$\frac{d\alpha}{dt} = r_1(\alpha) + r_2(\alpha); \quad r_1(\alpha) = k_1(T)(1 - \alpha)^{n_1} \tag{8}$$

$$r_2(\alpha) = k_2(T)\alpha^{n_2}(1 - \alpha)^{n_3}$$

where r_1 and r_2 are rates of stage one and two; and n_3 is reaction order of stage three.

The kinetic evaluation parameters were computed by the experimental data from DSC tests. In particular, the hypothesized TBPB’s thermal decomposition belongs to an unknown reaction, such as n th order or autocatalytic reaction. Comparisons of n th order and autocatalytic simulation computed the thermokinetic parameters. The two types of simulation results of thermokinetic parameters were evaluated as presented in Tables 3 and 4.

In contrast to Tables 3 and 4, which found n th order simulation results, E_a value can be matched to the Kissinger and Ozawa–Flynn–Wall kinetic algorithms. Thus, from the results of simulation for n th order and autocatalytic, this study obtained a better condition applying TBPB’s thermal explosion parameter evaluation by n th order simulation. Moreover, comparisons of experimental data and n th order simulated for heat production (Q_0) versus time, and heat production rate (Q_t) versus time are delineated in Figs. 5 and 6, respectively. TBPB’s TMR_{iso} , TER , and TCL were acquired at various scanning rates as shown in Table 5.

Table 4 Thermokinetic parameters evaluated by autocatalytic simulation

Sample	TBPB				
	$\beta/^\circ\text{C min}^{-1}$	1	2	4	10
$\ln k_0/\ln \text{sec}^{-1}$		22.22	22.10	20.76	22.19
$E_a/\text{kJ mol}^{-1}$		96.83	96.44	93.94	98.03
Reaction order/ n_1		1.39	1.19	0.94	1.21
Reaction order/ n_2		0.36	0.21	0.12	0.35
Autocatalytic constant/ z		0.06	0.03	0.60	0.58
$\Delta H_d/\text{kJ kg}^{-1}$		1,250.83	1,248.13	1,420.09	1,141.31

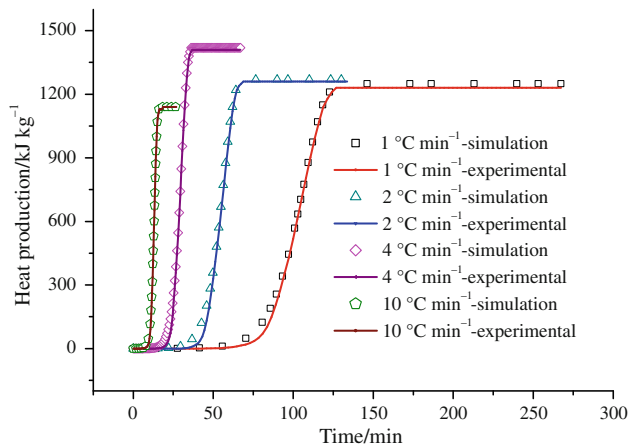


Fig. 5 Comparisons of TBPB's Q_0 versus time curves of n th order reaction with scanning rates of 1, 2, 4, and $10^\circ\text{C min}^{-1}$ by experimental and simulation

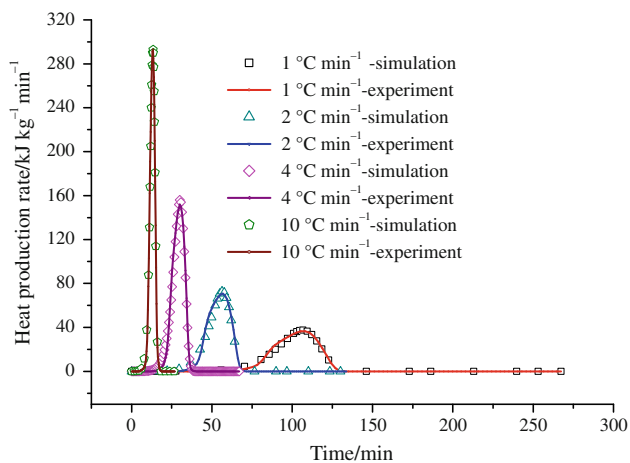


Fig. 6 Comparisons of TBPB's Q_1 versus time curves of n th order reaction at scanning rates of 1, 2, 4, and $10^\circ\text{C min}^{-1}$ by experimental and simulation

From Table 5, TBPB's TMR_{iso} exceeds the upper limit ca. 5 min at 100°C , and TCL is greater than upper limit 0.02 days at 100°C , which then could be applied afterward on the ambient temperature setup condition for

Table 5 TMR_{iso} , TER , and TCL at scanning rates of 1, 2, 4, and $10^\circ\text{C min}^{-1}$ by n th order simulation

$\beta/^\circ\text{C min}^{-1}$	1				2				4				10			
	Temperature/ $^\circ\text{C}$	$TMR_{iso}/$ min	$TER/$ kJ kg^{-1}	TCL/day ($CL = 10\%$)	$TMR_{iso}/$ min	$TER/$ kJ kg^{-1}	TCL/day ($CL = 10\%$)	$TMR_{iso}/$ min	$TER/$ kJ kg^{-1}	TCL/day ($CL = 10\%$)	$TMR_{iso}/$ min	$TER/$ kJ kg^{-1}	TCL/day ($CL = 10\%$)	$TMR_{iso}/$ min	$TER/$ kJ kg^{-1}	TCL/day ($CL = 10\%$)
20	68387.51	1.24E+03	1.27E+03	483.39	49124.1	1.27E+03	348.36	38789.45	1.42E+03	299.02	71516.75	1.13E+03	462.53	24604.09	1.13E+03	151.22
27.27	23461.84	1.24E+03	1.27E+03	157.62	17144.5	1.27E+03	115.55	13633.2	1.42E+03	99.89	8913.81	1.13E+03	52.12	8913.81	1.13E+03	52.12
34.55	8477.28	1.24E+03	1.27E+03	54.19	6296.69	1.27E+03	40.38	5040.73	1.42E+03	35.14	3388.49	1.13E+03	18.87	3388.49	1.13E+03	18.87
41.82	3214.3	1.24E+03	1.27E+03	19.57	2424.98	1.27E+03	14.81	1953.72	1.42E+03	12.98	1347.14	1.13E+03	7.15	1347.14	1.13E+03	7.15
49.09	1274.75	1.24E+03	1.27E+03	7.4	976.13	1.27E+03	5.69	791.24	1.42E+03	5.01	558.45	1.13E+03	2.83	558.45	1.13E+03	2.83
56.36	527.2	1.24E+03	1.27E+03	2.92	409.48	1.27E+03	2.28	333.86	1.42E+03	2.02	240.74	1.13E+03	1.17	240.74	1.13E+03	1.17
63.64	226.75	1.24E+03	1.27E+03	1.2	178.53	1.27E+03	0.95	146.37	1.42E+03	0.85	107.65	1.13E+03	0.5	107.65	1.13E+03	0.5
70.91	101.17	1.24E+03	1.27E+03	0.51	80.7	1.27E+03	0.41	66.52	1.42E+03	0.37	49.81	1.13E+03	0.22	49.81	1.13E+03	0.22
78.18	46.72	1.24E+03	1.27E+03	0.23	37.74	1.27E+03	0.18	31.26	1.42E+03	0.17	23.81	1.13E+03	0.1	23.81	1.13E+03	0.1
85.45	22.28	1.24E+03	1.27E+03	0.1	18.21	1.27E+03	0.08	15.16	1.42E+03	0.08	11.73	1.13E+03	0.05	11.73	1.13E+03	0.05
92.73	10.95	1.24E+03	1.27E+03	0.05	9.06	1.27E+03	0.04	7.58	1.42E+03	0.04	5.94	1.13E+03	0.02	5.94	1.13E+03	0.02
100	5.54	1.24E+03	1.27E+03	0.02	4.63	1.27E+03	0.02	3.89	1.42E+03	0.02						

liquid thermal explosion simulation under various storage conditions. While analyzing TBPB’s thermokinetic parameters by TSS, we obtained four numbers of thermokinetic parameters in various scanning rates at 1, 2, 4, and 10 °C min⁻¹ applied on the thermal explosion simulation.

Liquid thermal explosion simulation

To simulate thermal explosions in liquid, the critical parameters of thermal explosion are found numerically in the context of complicated chemical kinetics for several types of the reactor geometry, various boundary conditions, and with the possibility to set inert partitions or shells. For liquid thermal explosion simulation, there are the following equations [12, 27]:

$$\rho C_p \frac{\partial T}{\partial t} = \text{div}(\lambda \Delta T) + W \tag{9}$$

Thermal conductivity equation

$$\frac{\partial \alpha_i}{\partial t} = r_i \quad i=1, \dots, NC \quad \text{Kinetic equations (formal models)} \tag{10}$$

$$W = \sum_{(i)} Q_i^\infty r_i \quad \text{Heat power equation} \tag{11}$$

where *T* is the temperature; *t* is the time; ρ is the density; *C_p* is the specific heat; λ is the thermal conductivity; *Q_i[∞]* is the reaction calorific effect; *W* is the heat power; *r* is the reaction rate; α is the degree of conversion of a component; *NC* is the number of components; and *i* is the component number.

Initial fields of the temperature and conversions are supposed to be constant through the reactor volume:

$$\begin{aligned} T|_{t=0} &= T_0 \\ \alpha_i|_{t=0} &= \alpha_{i0} \end{aligned} \tag{12}$$

Here, the index 0 marks initial values of the temperature and conversion. The boundary conditions of the first, second, or third kind can be specified:

$$\text{1st kind : } T|_{\text{wall}} = T_e(t) \quad \text{Temperature} \tag{13}$$

$$\text{2nd kind : } q|_{\text{wall}} = q(t) \quad \text{Heat flow} \tag{14}$$

$$\text{3rd kind : } -\lambda \frac{\partial T}{\partial n} \Big|_S = \chi(T_{\text{wall}} - T_e) \tag{15}$$

Newton’s law of heat exchange

Here, the indices “wall” and “e” relate to the parameters on the boundary and the environment, respectively; *q* is the heat flow; and *n* is the unit outer normal on the boundary [11].

Table 6 Boundary condition for a 5-ton barrel reactor

Boundary conditions	$\chi/W \text{ m}^{-2} \text{ K}^{-1}$	Initial temperature/°C	Ambient temperature/°C			
Top/3rd kind	10	20	37	60	120	250
Side/3rd kind	10	20	37	60	120	240
Bottom/1st kind	–	20	20	20	20	20

Determination of TBPB’s liquid thermal explosion parameters

According to a 5-ton barrel reactor experimental setup, the TBPB ambient temperature of the seal of reactor is ca. 37 °C under room temperature in summer but is ca. 60 °C in outdoor exposure under sunlight, the overheating environment temperature and the temperature for the scene of the fire are 120 °C, and 250 °C, respectively. Runaway reaction simulation of boundary condition for a 5-ton barrel reactor is listed in Table 6; the runaway reaction graphics and the thermal hazard 3D graphs (only displaying scanning rate for 1 °C min⁻¹ condition) are illustrated in Figs. 7, 8, 9, 10. Comparisons of the literatures and simulation for TBPB’s *SADT*, *CT*, *ET*, and *TCR* are presented in Table 7. From Table 7, we acquired TBPB’s thermal decomposition stability in small reactors, as better than that of the 5-ton reactor at lower ambient temperature. We can see again that the larger the reactor, the smaller the *SADT* that will have inferior stability and applicability.

Therefore, the analysis of thermokinetic parameters of the thermal decomposition of TBPB depended on the reliability of the kinetic model. We applied the Kissinger and Ozawa–Flynn–Wall kinetic equation for the evaluation of thermokinetic parameters and compared the results to simulated thermal analysis. This approach led to the development of a precise and effective procedure for the evaluation of thermal decomposition properties of TBPB. Moreover, we discovered a rapid way to analyze thermokinetic parameters for organic peroxides such as TBPB. Furthermore, we obtained an efficient procedure for determining thermokinetic parameters and thermal hazard characteristics of TBPB that could be applied as a reduction of energy potential, and safer design during relevant operations and storage conditions.

Many excellent studies that have focused on thermal analysis and organic peroxides have been conducted and proposed by scientists all around the world (Fisher and Goetz [15, 16], Whitmore and Wilberforce [17, 18], Malow and Wehrstedt [19], Kotoyori [20], Sun et al. [21], Yang et al. [22], Yu and Hasegawa [23], Li and Hasegawa [24], Hordijk and Groot [25], Roduit et al. [26], etc.). We sincerely hope that this study can help the concerned plants to effectively avoid runaway or explosive accidents.

Fig. 7 Liquid thermal explosion simulation by runaway reaction graphs of TBPB with a barrel reactor at ambient temperature 37 °C: runaway reaction curve at various scanning rates of 1, 2, 4, and 10 °C min⁻¹ and 3D graph

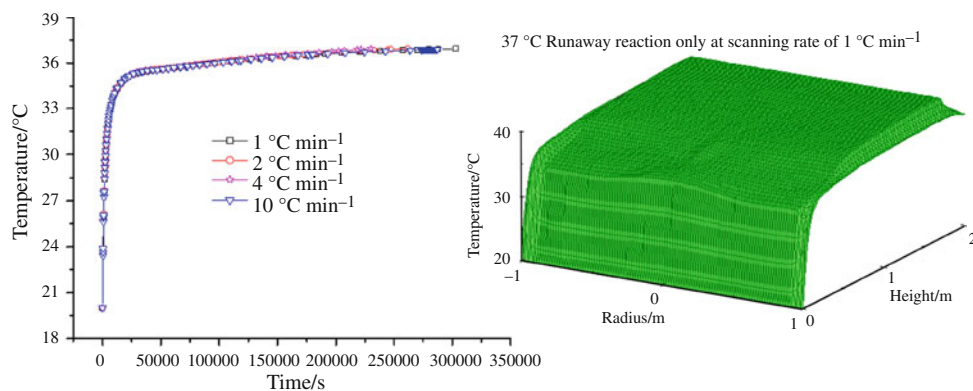


Fig. 8 Liquid thermal explosion simulation by runaway reaction graphs of TBPB with a barrel reactor at ambient temperature 60 °C: runaway reaction curve at various scanning rates 1, 2, 4, and 10 °C min⁻¹ and 3D graph

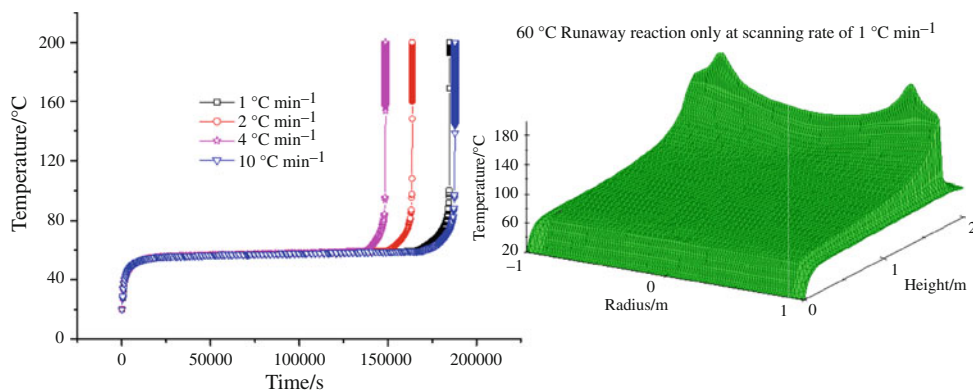


Fig. 9 Liquid thermal explosion simulation by runaway reaction graphs of TBPB with a barrel reactor at ambient temperature 120 °C: runaway reaction curve at various scanning rates of 1, 2, 4, and 10 °C min⁻¹ and 3D graph

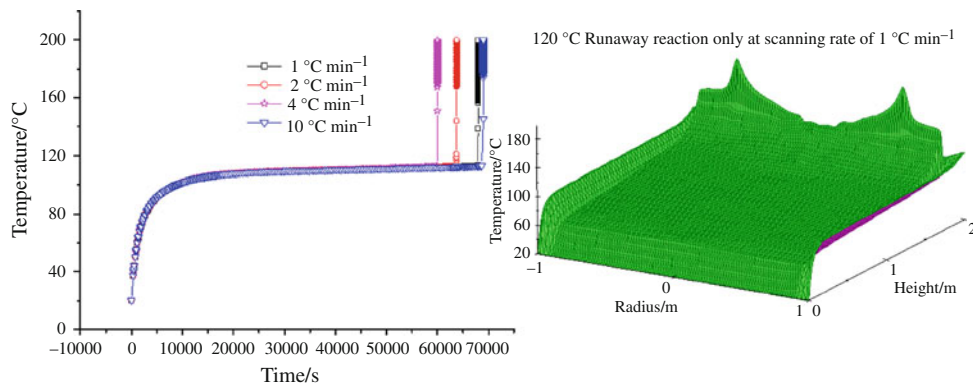


Fig. 10 Liquid thermal explosion simulation by runaway reaction graphs of TBPB with a barrel reactor at ambient temperature 250 °C: runaway reaction curve at various scanning rates of 1, 2, 4, and 10 °C min⁻¹ and 3D graph

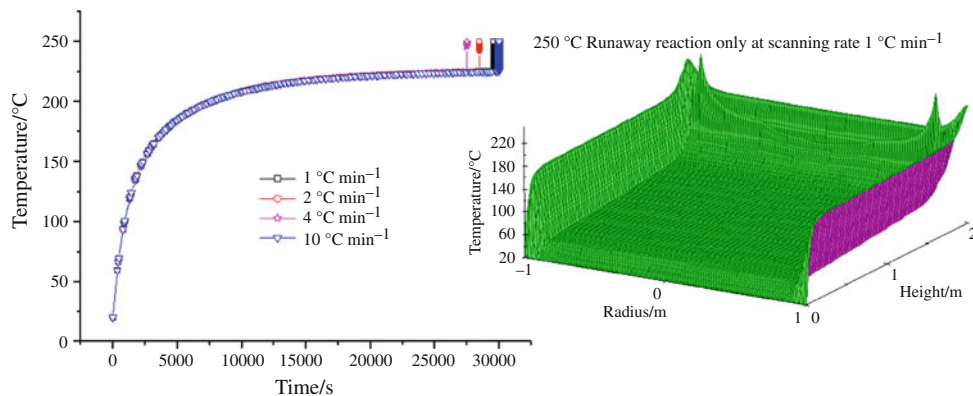


Table 7 Comparisons of the literature and liquid thermal explosion simulation for TBPB's *SADT*, *CT*, *ET*, and *TCR* at scanning rates of 1, 2, 4, and 10 °C min⁻¹ under a 5-ton reactor condition

Size	Test method or DSC scanning rate of this study	<i>SADT</i> / °C	<i>CT</i> / °C	<i>ET</i> / °C	<i>TCR</i> / °C
0.5-L vessel	UN test, Dewar test	60 ^a , 64 ^b , 65 ^c	-	-	-
	Heat flux calorimeter (Setaram C80D)	57 ^{b,d}	-	-	-
25-kg package	Accelerating rate calorimeter (ARC)	53 ^{e,f}	-	-	-
	US test	57 ^{e,f}	-	-	-
5-ton reactor	1	43	33	38	41.7
	2	41	31	36	39.7
	4	39	29	34	37.7
	10	43	33	38	43

^a Akzo Nobel [1]^b Yu and Hasegawa [23]^c Malow and Wehrstedt [19]^d Li and Hasegawa [24]^e Fisher and Goetz [15, 16]^f Wilberforce [17]

Conclusions

A huge reactor or package for thermokinetic parameters and thermal hazard of TBPB in the simulation was studied. Modeling TBPB's thermokinetic parameters and safety parameters precisely provided information on hazards, and on how to avoid accidents during transportation or storage. We established a green thermal analysis technology on thermokinetic and thermal hazard parameters of TBPB for the simulation method. We also discovered that a huge reactor or package applied on operations and storage conditions is very dangerous for organic peroxides. This study describes a highly delicate method to assess the thermokinetic parameters for TBPB. Data processing, kinetics evaluation, and estimation of k_0 , n , E_a , *CT*, *TCR*, *ET*, ΔH_d , *SADT*, *TCL*, *TER*, and TMR_{iso} , etc., were obtained by green analysis technology.

Acknowledgements The authors are indebted to Mr. Yu-Chuan Chou for technical suggestions on experiments and analyses of TBPB thermal properties. In addition, the authors are grateful to Yuh Tzong Enterprise Ltd. in Taiwan, ROC.

References

- Material safety data sheet. Akzo Nobel Chemicals bv Stationsplein 4. P.O. Box 247, 3800 AE Amersfoort, The Netherlands; 2007.
- NFPA 432. Code for the storage of organic peroxide formulations. Quincy, MA, National Fire Protection Association, 2008.
- STAR[®] Software with Solaris Operating System, Operating Instructions; Mettler Toledo: Sweden, 2004.
- Lin CP, Shu CM. A comparison of thermal decomposition energy and nitrogen content of nitrocellulose in non-fat process of linters by DSC and EA. *J Therm Anal Calorim*. 2009;95:547–52.
- Kissinger HE. Reaction kinetics in differential thermal analysis. *Anal Chem*. 1957;29:1702–6.
- Ozawa T. A new method of analyzing thermogravimetric data. *Bull Chem Soc Jpn*. 1965;38:1881–6.
- Ozawa T. Kinetic analysis of derivative curves in thermal analysis. *J Therm Anal*. 1970;2:301–24.
- Ozawa T. Estimation of activation energy by isoconversion methods. *Thermochim Acta*. 1992;203:159–65.
- Ozawa T. Thermal analysis-review and prospect. *Thermochim Acta*. 1999;355:35–42.
- Flynn JH, Wall LA. A quick, direct method for the determination of activation energy from thermogravimetric data. *J Polym Sci B*. 1966;4(5):323–8.
- Thermal safety software (TSS). St. Petersburg, Russia: ChemInform Saint-Petersburg (CISP) Ltd., <http://www.cisp.spb.ru>.
- Recommendations on the transport of dangerous goods, manual of tests and criteria, 4th rev. ed. New York, United Nations: 2003.
- Recommendations on the transport of dangerous goods, model regulations, 16th rev. ed. New York, United Nations: 2009.
- European agreement concerning the international carriage of dangerous goods by road (ADR). New York, United Nations: 2009.
- Fisher HG, Goetz DD. Determination of self-accelerating decomposition temperatures using the accelerating rate calorimeter. *J Loss Prev Process Ind*. 1991;4:305–16.
- Fisher HG, Goetz DD. Determination of self-accelerating decomposition temperatures for self-reactive substances. *J Loss Prev Process Ind*. 1993;6(3):183–94.
- Wilberforce JK. The use of the accelerating rate calorimeter to determine the *SADT* of organic peroxides. Internal report. Texas: Columbia Scientific Corporation, 1981.
- Whitmore MW, Wilberforce JK. Use of the accelerating rate calorimeter and the thermal activity monitor to estimate stability temperatures. *J Loss Prev Process Ind*. 1993;6(2):95–101.
- Malow M, Wehrstedt KD. Prediction of the self-accelerating decomposition temperature (*SADT*) for liquid organic peroxides from differential scanning calorimetry (DSC) measurements. *J Hazard Mater*. 2005;A120:21–4.
- Kotoyori T. Critical temperatures for the thermal explosion of liquid organic peroxides. *Process Saf Prog*. 1995;14(1):37–44.
- Sun JH, Li YF, Hasegawa K. A study of self-accelerating decomposition temperature (*SADT*) using reaction calorimetry. *J Loss Prev Process Ind*. 2001;14(5):331–6.
- Yang D, Koseki H, Hasegawa K. Predicting the self-accelerating decomposition temperature (*SADT*) of organic peroxides based on non-isothermal decomposition behavior. *J Loss Prev Process Ind*. 2003;16(5):411–6.
- Yu YH, Hasegawa K. Derivation of the self-accelerating decomposition temperature for self-reactive substances using isothermal calorimetry. *J Hazard Mater*. 1996;45(2–3):193–205.
- Li YF, Hasegawa K. On the thermal decomposition mechanism of self-accelerating materials and the evaluating method for their *SADTs*. In: Ninth international symposium on loss prevention and safety promotion in the process industries. Spain, p. 555–69, 1998.
- Hordijk AC, Groot JJ. Experimental data on the thermal kinetics of organic peroxides. *Thermochim Acta*. 1986;101:45–63.
- Roduit B, Folly P, Berger B, Mathieu J, Sarbach A, Andres H, Ramin M, Vogelsanger B. Evaluating *SADT* by advanced kinetics-based simulation approach. *J Therm Anal Calorim*. 2008;93(1):153–61.
- Frank-Kamenetskii DA. Diffusion and heat exchange in chemical kinetics. 2nd ed. New York: Plenum Press; 1969.